

- were inspected under $\times 10$ magnification, and 200 to 300 mg were selected for the mass spectrometric analyses. Details of the chemical and instrumental procedures were reported in (6).
10. Stratigraphic sections are presented by D. R. Muhs and B. J. Szabo [*Mar. Geol.* **118**, 315 (1994)]. The normal tidal range of Oahu is < 0.8 m, and modern coral reefs in protected bays grow upward to ~ 0.5 m below low tide level.
 11. R. L. Edwards *et al.* [*Science* **260**, 962 (1993)] reported that the variation in the initial $^{234}\text{U}/^{238}\text{U}$ activity value in 20 young (1.8 to 13.1 ka) New Guinea corals did not exceed 2 per mil, or 1.150 ± 0.002 (2σ of population). Our measurements of 16 young (modern to 16 ka) Florida and Hawaii corals yield a value of 1.148 ± 0.002 (2σ of the mean) (K. R. Ludwig, K. R. Simmons, D. R. Muhs, B. J. Szabo, unpublished data). For the purpose of this report, we specify an acceptable range of variation for initial $^{234}\text{U}/^{238}\text{U}$ of 1.146 to 1.150. The range of U concentrations of the Oahu corals is 2.31 to 3.96 ppm, and the range of U concentrations in young Hawaiian corals (< 15 ka) is 2.39 to 3.15 ppm [K. R. Ludwig, B. J. Szabo, J. G. Moore, K. R. Simmons, *Geology* **19**, 171 (1991); this report]; we do not have large deviations indicative of an open system. All of the fossil Oahu corals have $^{230}\text{Th}/^{232}\text{Th}$ activity ratios of > 800 , indicating that the samples should be free of inherited ^{230}Th from detrital materials. However, we cannot rule out the possibility that a minute amount of ^{230}Th , derived from dissolution of existing nearby coral, may have been incorporated into some of our samples, causing the calculated ages to be too old.
 12. M. Stein *et al.*, *Geochim. Cosmochim. Acta* **57**, 2541 (1993).
 13. C. D. Gallup, R. L. Edwards, R. G. Johnson, *Science* **263**, 796 (1994). According to their model, category B equivalent ages are accurate to within < 2000 years.
 14. Arbitrary age estimates based on the observation that the apparently sharp cutoff in all category A and category B ages at about 131 and 114 ka, respectively, is about what one would expect for a true range of 131 to 114 ka, allowing for some dispersion at the extremes from analytical error.
 15. A. L. Berger, *Quat. Res.* **9**, 139 (1978); _____ and M. F. Loutre, *Quat. Sci. Rev.* **10**, 297 (1991).
 16. D. Rind, D. Peteet, G. Kukla, *J. Geophys. Res.* **94** (no. D10), 12851 (1989). Climate modeling experiments using the most favorable insolation variations have also failed to predict that snow cover could be maintained or the growth of major ice sheets initiated at northern latitudes, despite the major reduction in insolation culminating at 116 ka.
 17. Unexplained aspects associated with the 10^5 -year cycle responding to the orbital climate forcing are examined by J. Imbrie *et al.* [*Paleoceanography* **8**, 699 (1993)], and the internal response to orbital forcing is discussed by N.-A. Mörner [in *Orbital Forcing and Cyclic Sequences*, P. L. de Boer and D. G. Smith, Eds. (Special Publication of the International Association of Sedimentologists, Blackwell Scientific, Oxford, 1994), no. 19, pp. 25–33]. Changes in the Earth's geoid may have affected local paleosea level conditions [K. Lambeck and M. Nakada, *Nature* **357**, 125 (1992); A. Eisenhauer *et al.*, *Earth Planet. Sci. Lett.* **114**, 529 (1993)].
 18. L. B. Collins *et al.*, *Mar. Geol.* **110**, 203 (1993); Z. R. Zhu *et al.*, *Earth Planet. Sci. Lett.* **118**, 281 (1993).
 19. R. L. Edwards, J. H. Chen, T.-L. Ku, G. J. Wasserburg, *Science* **236**, 1547 (1987); B. Hamelin, E. Bard, A. Zindler, R. G. Fairbanks, *Earth Planet. Sci. Lett.* **106**, 169 (1991).
 20. C. E. Stearns, *Quat. Res.* **6**, 445 (1976); J. Chappell and H. H. Veeh, *Geol. Soc. Am. Bull.* **89**, 356 (1973); P. L. Smart and D. A. Richards, *Quat. Sci. Rev.* **11**, 687 (1992).
 21. C. E. Sherman *et al.*, *Geology* **21**, 1079 (1993).
 22. H. T. Stearns, *Bernice P. Bishop Mus. Bull.* **237**, 1 (1978); *Geology of the State of Hawaii* (Pacific Books, Palo Alto, CA, 1966).
 23. Large submarine landslides have been mapped adjacent to the islands of Hawaii including Oahu [J. G. Moore, W. R. Normark, R. T. Holcomb, *Science* **264**, 46 (1994); J. G. Moore *et al.*, *J. Geophys. Res.* **94**, 17465 (1989)]. Some of these debris avalanches may have produced giant wave deposits on the coastal slopes of Molokai and Lanai [J. G. Moore, W. B. Bryan, K. R. Ludwig, *Geol. Soc. Am. Bull.* **106**, 962 (1994); J. G. Moore and G. W. Moore, *Science* **226**, 1312 (1984)]. We studied the exposures of the ~ 30 -m Kaena reef deposits about 3 km southeast of Kaena Point (SKP in Fig. 1) and found no sedimentological characteristics that suggest an origin from a giant wave. Furthermore, morphologic analysis of nick points on interfluvial suggests the existence of a former shoreline with a mean elevation of about 28 m [R. V. Ruhe, J. M. Williams, E. L. Hill, *J. Geol.* **73**, 485 (1965)].
 24. M. A. Lanphere and G. B. Dalrymple, *Am. J. Sci. A* **280**, 736 (1980); H. T. Stearns and G. B. Dalrymple, *Bernice P. Bishop Mus. Occas. Pap.* **24**, 307 (1978).
 25. H. T. Stearns, *Geol. Soc. Am. Bull.* **85**, 795 (1974).
 26. E. Bard, B. Hamelin, R. G. Fairbanks, *Nature* **346**, 456 (1990).
 27. P. de Bièvre *et al.*, in *Proceedings of the International Conference on Chemical and Nuclear Data: Measurements and Applications*, M. L. Hurrell, Ed. (Institute of Civil Engineers, London, 1971), pp. 211–225; J. W. Meadows, R. J. Armani, E. L. Callis, A. M. Essling, *Phys. Rev. C* **22**, 750 (1980).
 28. We thank G. R. Bauer and J. G. Moore, who provided assistance in the sample collection. This report benefited from review comments by I. Winograd and T. McConnaughey. We thank S. Allison for allowing us access to his property. This paper is a contribution to the LITE (Last Interglacial: Timing and Environment) project of the Global Change and Climate History Program of the U.S. Geological Survey.

17 May 1994; accepted 8 August 1994

Interannual Variability of Temperature at a Depth of 125 Meters in the North Atlantic Ocean

Sydney Levitus,* John I. Antonov,† Timothy P. Boyer

Analyses of historical ocean temperature data at a depth of 125 meters in the North Atlantic Ocean indicate that from 1950 to 1990 the subtropical and subarctic gyres exhibited linear trends that were opposite in phase. In addition, multivariate analyses of yearly mean temperature anomaly fields between 20°N and 70°N in the North Atlantic show a characteristic space-time temperature oscillation from 1947 to 1990. A quasidecadal oscillation, first identified at Ocean Weather Station C, is part of a basin-wide feature. Gyre and basin-scale variations such as these provide the observational basis for climate diagnostic and modeling studies.

Levitus *et al.* (1) presented analyses of temperature time series data at Ocean Weather Station C (OWS C) that indicated the interannual variability of upper ocean thermal structure at this location during the period from 1947 through 1990. The presence of two distinct signals in the data, a temperature oscillation with a quasidecadal time scale and a linear decrease in the data from 1956 through 1985 (Fig. 1), raised the question of the geographical extent and temporal variability of these features. In this report we address these questions by analyzing data collected in the North Atlantic from 20°N to 70°N .

There is little observational evidence of basin- and gyre-scale temperature variability at subsurface depths for any part of the world ocean for interannual to decadal time scales. Such variability, as we identify in this report, is important to the understanding of climate change because of air-sea interactions that may be involved in this variability. The identification of such vari-

ability can provide the basis for diagnostic studies and modeling simulations, as well as for the development of a monitoring strategy for the ocean. With present concern about the possibility of global warming, the identification and understanding of thermal variability in the ocean, whether natural or anthropogenic, is an important subject of study.

We have used historical oceanographic measurements of temperature to analyze the variability of temperature (2) at a depth of 125 m in the North Atlantic Ocean. These data include both time series data from OWS C (3) and historical data from the entire North Atlantic. We analyzed data at a depth of 125 m because this is the deepest standard observation level for which data exist as far back as 1947 for the North Atlantic between 20°N and 70°N . These early data are primarily mechanical bathythermograph (MBT) observations. In addition, the annual cycle of temperature at this depth is relatively small compared to that at the sea surface. Thus, we can expect that the greater part of variability at this depth is associated with temperature variations at periods of more than a year. Yearly data distributions at a depth of 125 m show the data to be variable in space and time; more data are available along the boundary of the Atlantic than in the interior region, and more data are

S. Levitus and T. P. Boyer, National Oceanographic Data Center, E/OC5, Universal Building, 1825 Connecticut Avenue, NW, Washington, DC 20235, USA.

J. I. Antonov, State Hydrological Institute, 23 Second Lane, B.O., St. Petersburg, Russia 199053.

*To whom correspondence should be addressed.

†Present address: National Oceanic and Atmospheric Administration—National Oceanographic Data Center, Ocean Climate Laboratory, Universal Building, 1825 Connecticut Avenue, NW, Washington, DC 20235, USA.

available during recent years than earlier (2).

In order to prepare estimates of the variability of upper ocean thermal structure for the world ocean (within the limits of available data), we used all historical temperature profiles including reversing thermometers, MBTs, expendable bathythermographs (XBTs) (corrected for a drop-rate error) and conductivity (salinity)-temperature-depth (C/STDs) data (2). First, we subtracted the climatological monthly mean temperatures from the values at the standard observation level in each profile. Next, we composited all historical temperature data by individual years on a 1° latitude-longitude grid at standard observation levels. Finally, we analyzed the composited temperature anomaly 1° -square means for each year, using objective analysis techniques (2, 4). Features with wavelengths less than 1000 km are substantially smoothed by this scheme.

As shown by Levitus *et al.* (1), annual mean temperatures from OWS C at a depth of 125 m for 1946 to 1985 decreased linearly by approximately 0.13°C per decade (Fig. 1). In addition, there is a quasidecadal-scale oscillation with a range of about 2.0°C and peaks occurring in 1956, 1965, and 1979. The years for which we have both station data and MBT data indicate good agreement between these two sets of measurements. This agreement gives us confidence in the accuracy and representativeness of the MBT data that are averaged as we have done (1). The signal (2°C peak-to-trough difference in annual mean temperature) in Fig. 1 is more than twice the 1°C range of the annual cycle at this depth.

The mapping of temperature anomalies in the North Atlantic for each year shows that certain anomaly patterns repeat over a relatively large part of the North Atlantic Ocean. In addition, anomalies in the same region oscillate in sign with multiyear periods. To investigate these irregular oscillations statistically, we analyzed the anomalies using the empirical orthogonal function (EOF) technique (5) on a 5° latitude by 15° longitude grid for 1947 to 1990.

The first EOF (not shown) accounts for approximately 32% of the variance of interannual temperature variability at a depth of 125 m. It has a simple dipole structure. On the basis of the geographical locations of the dipole centers and the dividing zero line, this EOF can be interpreted as an opposition between subarctic and subtropical gyres. In other words, about one-third of the total variance can be accounted for by the fact that the sign of the temperature anomalies in the subarctic gyre was opposite that of the anomalies in the subtropical gyre during the period from 1947 through 1990.

The time series of the first EOF shows how the amplitude of this dipole structure changed in time. Only 30% of the temporal variability of this EOF can be accounted for

by the linear trend for the whole period because the linear trend changed its sign around the mid-1960s. Temporal variability of this pattern can be interpreted as a cool-

Fig. 1. Time series of annual mean temperature (in degrees Celsius) at a depth of 125 m from OWS C ($52^\circ45'\text{N}$, $35^\circ30'\text{W}$) data. The annual means are computed as the average of the available monthly means for each year. Each monthly mean is computed as the average of all daily mean profiles in each month. All years plotted had at least one monthly mean from each of the four seasons. The vertical bars centered at each annual mean represent plus and minus one standard error of the monthly means in each year about the annual mean for that year.

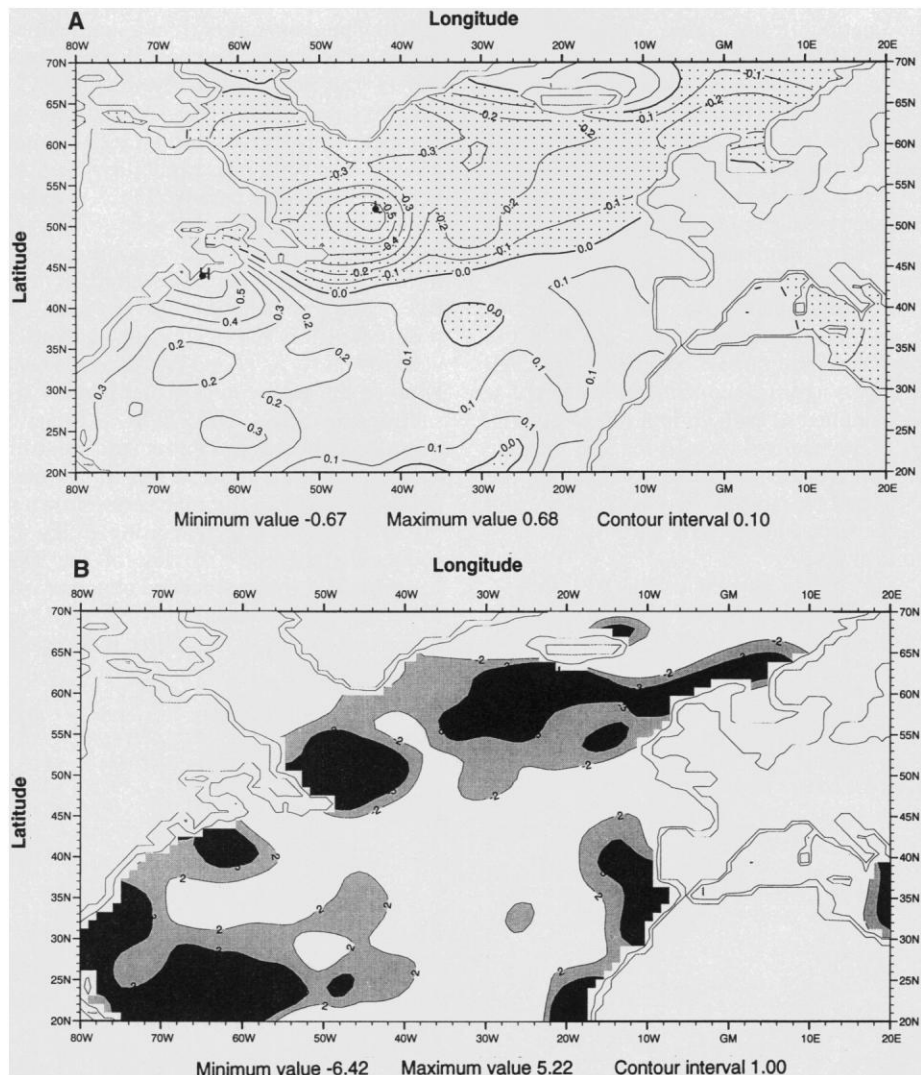
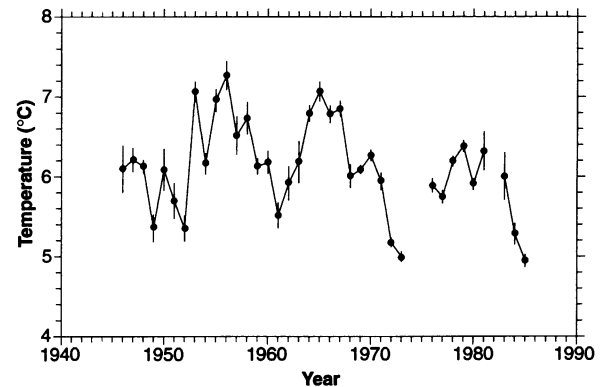


Fig. 2. (A) Linear trend (in degrees Celsius per decade) of temperature at a depth of 125 m from 1966 to 1990. The estimates are based on a 1° latitude-longitude gridded time series of temperature anomalies. (B) Statistical significance of the linear trend temperature estimates at a depth of 125 m from 1966 to 1990 based on a two-tailed Student's *t* test. Black regions correspond to a 99% significance level, shaded regions to 95%.

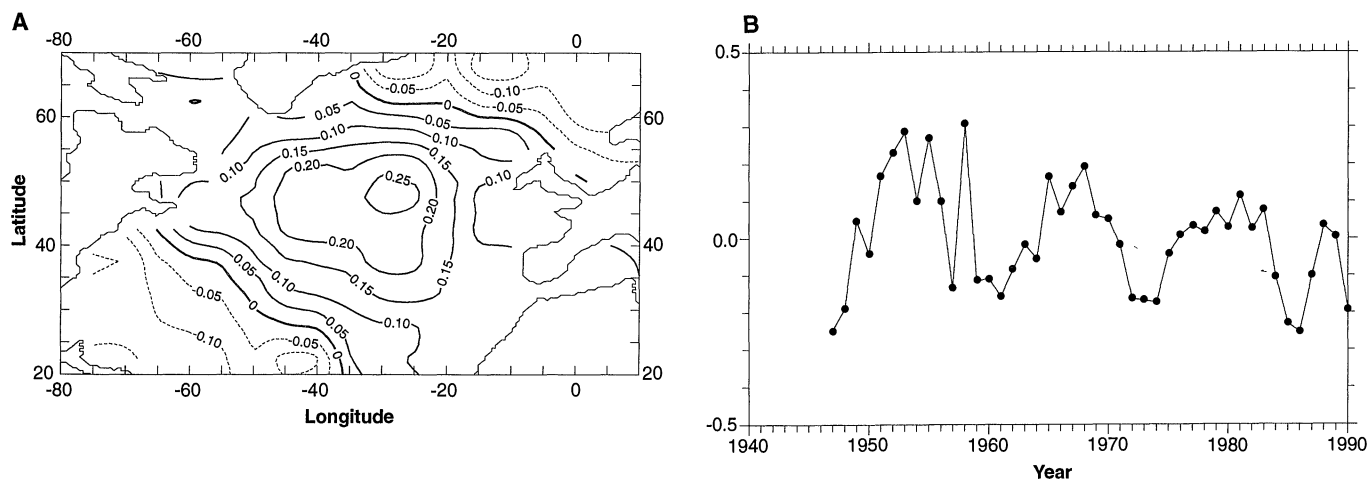


Fig. 3. (A) Loading pattern for the second EOF of the temperature anomalies at a depth of 125 m. (B) Time series of the second EOF loading pattern.

ing of much of the subtropical gyre and a warming of part of the subarctic gyre during the period from 1954 through 1965. Around 1966 the signs of these trends reversed. The geographical distribution of the linear trend for the period from 1966 to 1990 is shown in Fig. 2A. We present estimates of the trend for this period because its pattern is similar to that of the first EOF and because such a signal is of interest in its own right. The temperature increased by more than 0.2°C per decade west of 50°W in the subtropical gyre and decreased by about the same value west of 20°W in the subarctic gyre from 1966 to 1990 (Fig. 2A). A test of significance (Student's *t* test) has been applied to each gridpoint series in Fig. 2A. The results shown in Fig. 2B indicate that the trend patterns are significant at the 95% level for most of the subarctic gyre and the western and eastern parts of the subtropical gyre.

The dipole pattern of the first EOF is also derived if the EOF analysis is applied to the same data after linear detrending. This

means that the opposition between subarctic gyre and subpolar gyre could be an oscillating process (rather than a simple linear model) whose period is equal to, or exceeds, the 44-year period we analyzed.

The second EOF (Fig. 3A) accounts for approximately 15% of the variance of interannual temperature variability at this depth. The loading pattern (Fig. 3A) exhibits a negative region between 60°N and 70°N. A zero line extending southeastward from 45°N, 65°W separates another negative region from a large positive region. The positive region has its largest magnitude along 45°N to 50°N and encompasses nearly all of the subarctic gyre and parts of the subtropical gyre. This EOF exhibits a quasidecadal-scale variability (the spectrum in Fig. 3B has a peak of about 13 years) nearly identical to the time series shown in Fig. 1. Each of the remaining EOFs accounts for about 8% or less of the total variance, and their associated characteristic roots are nearly equal.

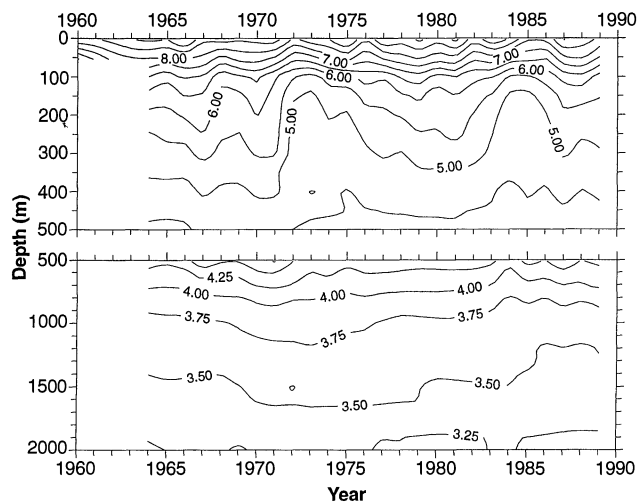
Earlier work (1) showed that the trend

and quasidecadal-scale oscillation of temperature at OWS C extended from the surface to a depth of 125 m. For the period from 1964 to 1990, temperature observations at OWS C were made to depths exceeding 2000 m (Fig. 4). The quasidecadal oscillations extend down to a depth of about 400 m for this period. In addition, a linear cooling trend is evident to depths of 1500 m and perhaps to a depth of 2000 m beginning in 1974, as evidenced by the rise in isotherms.

The time series results indicate that statistically significant decadal-scale changes of temperature have occurred in both the subarctic and subtropical gyres of the North Atlantic Ocean at a depth of 125 m. These results present further evidence of the variability of the thermohaline structure of the North Atlantic Ocean (6–16).

The variability that we have described possibly represents ocean components of interactions of the Earth's ocean-atmosphere-cryosphere climate system. The EOF loading pattern shown in Fig. 3A bears a remarkable resemblance to EOF loading patterns identified in sea-level pressure and air-sea heat flux patterns associated with an atmospheric oscillation of sea-level pressure known as the East Atlantic oscillation (17). We have computed EOFs of winter sea-surface pressure for the period from 1947 through 1990 and find an EOF whose loading pattern is very similar to that shown in Fig. 3A. The decadal component of the sea-level pressure time series is similar to that shown in Fig. 3B.

Fig. 4. Annual mean temperature (in degrees Celsius) to a depth of 2000 m at OWS C for 1964 to 1989.



REFERENCES AND NOTES

1. S. Levitus et al., in *Decadal-Scale Variability of the North Atlantic Ocean*, K. Bryan, Ed. (National Academy Press, Washington, DC, in press).
2. S. Levitus, T. Boyer, J. Antonov, *World Ocean Atlas 1994*, vol. 5: *Interannual Variability of Upper Ocean*

- Thermal Structure* [National Oceanic and Atmospheric Administration (NOAA) Atlas Series, Government Printing Office, Washington, DC, in press].
- Station OWS C was located (52.75°N, 35.5°W) in the subarctic gyre of the North Atlantic. This location is just north of the Ocean Polar Front, an upper ocean feature associated with the North Atlantic Current. From 1946 to 1973, OWS C was occupied by ships of the U.S. Coast Guard. From 1946 to 1964, temperature profiles were measured with MBT instruments. From 1964 through 1973, hydrographic casts (reversing thermometers to measure temperature and seawater samples gathered for salinity determinations) were made as well as MBT casts [see L. J. Hannon, "North Atlantic Ocean Station Charlie Terminal Report 1964-1973" (*Oceanographic Report CG 373-79*, U.S. Coast Guard Oceanographic Unit, Washington, DC, 1973)]. From 1975 through 1990, research ships from the former Soviet Union occupied this station. They took Nansen casts and salinity-temperature-depth profiles, in addition to some MBT profiles. Some of the former Soviet Union data taken at OWS C were available only in the form of daily means. Therefore, we averaged all data to obtain daily means before forming other averages so as to utilize all the former Soviet Union data and analyze all data in a consistent manner.
 - S. Levitus and T. P. Boyer, *World Ocean Atlas 1994*, vol. 4: *Temperature* (NOAA Atlas NESDIS 4, Government Printing Office, Washington, DC, 1994).
 - H. H. Harman, *Modern Factor Analysis* (Univ. of Chicago Press, Chicago, ed. 3, 1976); J. E. Jackson, *A User's Guide to Principal Components* (Wiley, New York, 1991).
 - J. R. N. Lazier, *Atmos. Ocean* **18**, 227 (1980); *Deep-Sea Res.* **35**, 1247 (1988); in *Decadal-Scale Variability of the North Atlantic Ocean*, K. Bryan, Ed. (National Academy Press, Washington, DC, in press).
 - P. G. Brewer *et al.*, *Science* **222**, 1237 (1983).
 - A. H. Taylor, *J. Climatol.* **3**, 253 (1983).
 - H. D. Dooley, J. H. A. Martin, D. J. Ellet, *Rapp. P.V. Reun. Cons. Int. Explor. Mer* **185**, 179 (1984).
 - D. Roemmich and C. Wunsch, *Nature* **307**, 447 (1984).
 - D. Roemmich, in *Glaciers, Ice Sheets, and Sea Level: Effect of a CO₂-Induced Climatic Change* (Department of Energy, Washington, DC, 1985), pp. 104-115.
 - J. H. Swift, in *Climatic Processes and Climate Sensitivity* (*Geophys. Monogr. Ser.* 29), J. E. Hansen and T. Takahashi, Eds. (American Geophysical Union, Washington, DC, 1984), pp. 39-47; in *Glaciers, Ice Sheets, and Sea Level: Effect of a CO₂-Induced Climatic Change* (Department of Energy, Washington, DC, 1985), pp. 129-138.
 - R. Dickson, J. Meinke, S. A. Malmberg, A. J. Lee, *Progr. Oceanogr.* **20**, 103 (1988).
 - J. Antonov and P. Groisman, *Meteorol. Hydrol.* **3**, 57 (1988) (in Russian).
 - S. Levitus, *J. Geophys. Res.* **94**, 6091 (1989); *ibid.*, p. 9679; *ibid.*, p. 16125; *ibid.* **95**, 5233 (1990).
 - J. Antonov, *Meteorol. Hydrol.* **4**, 78 (1990) (in Russian); J. Antonov, *J. Climate* **6**, 1928 (1993).
 - D. R. Cayan, *J. Phys. Oceanogr.* **22**, 859 (1992).
 - Funding for this work was provided by the NOAA Climate and Global Change Program and the NOAA Environmental Sciences Data and Information Management Program. This work was completed while J.A. was a research associate (National Research Council) at the National Oceanographic Data Center, NOAA, Washington, DC.

20 June 1994; accepted 18 August 1994

Atomic-Scale Dynamics of a Two-Dimensional Gas-Solid Interface

S. J. Stranick, M. M. Kamna, P. S. Weiss*

The interface between a two-dimensional (2D) molecular gas and a 2D molecular solid has been imaged with a low-temperature, ultrahigh-vacuum scanning tunneling microscope. The solid consists of benzene molecules strongly bound to step edges on a Cu{111} surface. Benzene molecules on the Cu{111} terraces move freely as a 2D gas at 77 kelvin. Benzene molecules transiently occupy well-defined adsorption sites at the 1D edge of the 2D solid. Diffusion of molecules between these sites and exchange between the two phases at the interface are observed. On raised terraces of the copper surface, the 2D gas is held in a cage of the solid as in a 2D nanometer-scale gas bulb.

The 2D phase diagram for adsorbates on surfaces has all of the complexity of the more familiar 3D analogs. Adsorbates can be found as 2D gases, liquids, and solids. Different 2D structures are formed as temperature and coverage are varied. A variety of scattering and diffraction techniques have been used to study the phase transitions of 2D systems (1). We report here observations of the atomic-scale dynamics of the equilibrium at the interface between a 2D solid and a 2D gas. We can record the motion of individual molecules at this interface, as has never been possible for 3D

systems. We used a low-temperature, ultrahigh-vacuum (UHV) scanning tunneling microscope (STM) (2) to observe these dynamics for benzene molecules adsorbed on the Cu{111} surface.

The STM has been used to analyze the kinetics of motion of surface adsorbates and surface features such as steps and vacancies (3-6). In making these measurements, researchers have used many of the methods earlier developed for quantifying motion on the atomic scale by field ion microscopy (7). For STM measurements, correlation techniques have been used to analyze images of mobile adsorbates at high surface coverages to determine favored adsorption sites, surface ordering, and interaction energies (8).

Weiss and Eigler have studied adsorption sites and their effects on STM images of isolated benzene molecules on Pt{111} at 4 K (9). At such a low temperature, benzene is frozen in place and no motion is observed. Benzene molecules have also been imaged on Rh{111} at room temperature when held fixed in various ordered overlayers by coadsorbed CO (10). On both Pt{111} and Rh{111} surfaces, benzene molecules lie flat, that is, with the molecular plane parallel to the surface plane. In another study of surface motion, Wolkow and Schofield used a low-temperature STM to observe the diffusion and perhaps desorption into the vacuum of isolated benzene molecules on the Si{111} surface (11).

After initial electrochemical polishing and repeated sputtering and annealing cycles in UHV, we obtained a clean flat Cu{111} crystal surface. We dosed the freshly cleaned crystal to saturation coverage at room temperature by bleeding a small amount of benzene gas through a sapphire leak valve into the vacuum chamber. We checked the purity of the benzene in situ by mass spectroscopy to verify that impurities and undesired wall reactions were negligible. After dosing, the room-temperature Cu{111} sample was rapidly transferred to a cryogenic UHV STM chamber held at 77 or 4 K (2).

Earlier studies by Bent and co-workers have shown that benzene adsorbs and desorbs molecularly on the Cu{111} surface (12). As for the close-packed Pt{111} and Rh{111} surfaces, the first monolayer of benzene adsorbs with the molecular plane parallel to the surface plane (12). From temperature-programmed desorption (TPD) of perdeutero (*d*₆) benzene on Cu{111}, multilayer and monolayer coverages of benzene are known to desorb from the surface below 250 K. A high-temperature tail in the TPD spectrum extending to 300 K is attributed to desorption from surface defect sites. Therefore, by dosing the Cu{111} crystal at room temperature with benzene, we preferentially populated defect sites such as step edges on the surface.

Initial STM observations showed that at both 4 and 77 K, the monatomic step edges on the Cu{111} surface were indeed decorated by adsorbed benzene. These features were not present in STM images of the bare Cu{111} surface. STM images of the benzene-covered surface recorded at 77 K are shown in Fig. 1, A and B. Both straight and meandering monatomic height steps are present on the Cu{111} surface (13), and all are decorated with benzene molecules. Because along straight steps benzene molecules order into well-defined adsorption sites, we concentrated our analysis on these step configurations.

At 77 K the benzene molecules are mo-

Department of Chemistry, Pennsylvania State University, University Park, PA 16802, USA.

*To whom correspondence should be addressed.